JCI insight

Mutations in *EPHB4* cause human venous valve aplasia

Oliver Lyons, … , Prakash Saha, Alberto Smith

JCI Insight. 2021. https://doi.org/10.1172/jci.insight.140952.

Research In-Press Preview Angiogenesis Development

Graphical abstract

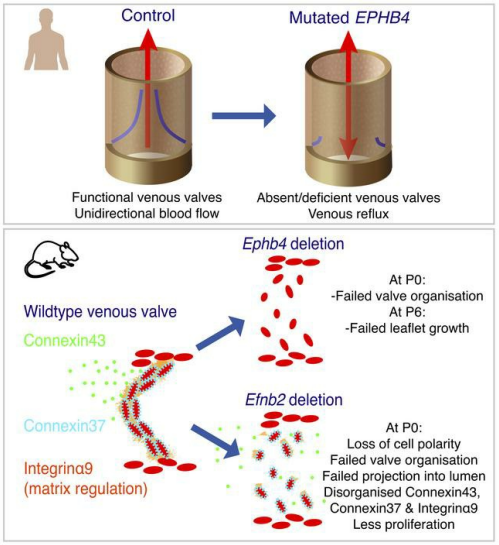

Find the latest version:

https://jci.me/140952/pdf

Title: Mutations in *EPHB4* cause human venous valve aplasia

Running Title: Venous valve aplasia

Authors

Oliver Lyons[1*], James Walker[1], Christopher Seet[1], Mohammed Ikram[1], Adam Kuchta[2], Andrew Arnold[2], Magda Hernandez-Vasquez[3], Maike Frye[3], Gema Vizcay-Barrena[4], Roland A. Fleck[4], Ash Patel[1], Soundrie Padayachee[2], Peter Mortimer[5], Steve Jeffery[5], Siren Berland[6], Sahar Mansour[5,7], Pia Ostergaard[5], Taija Makinen[3], Bijan Modarai[1], Prakash Saha[1], Alberto Smith[1 *]

Affiliations

1. Academic Department of Vascular Surgery, School of Cardiovascular Medicine and Sciences, BHF Centre of Research Excellence, King's College London, St Thomas' Hospital, London, United Kingdom
2. Department of Ultrasonic Angiology, Guy's & St Thomas' NHS Foundation Trust, London, United Kingdom
3. Rudbeck Laboratory, Department of Immunology, Genetics and Pathology, Uppsala University, Sweden
4. Centre for Ultrastructural Imaging, King's College London, London, United Kingdom
5. Molecular and Clinical Sciences Research Institute, St George's University of London, London, United Kingdom
6. Department of Medical Genetics, Haukeland University Hospital, Bergen, Norway
7. South West Thames Regional Genetics Service, St George's Hospital, London, United Kingdom

The authors have declared that no conflict of interest exists.

Corresponding authors

Dr Oliver Lyons & Prof Alberto Smith
Academic Department of Vascular Surgery, King's College London
1st Floor North Wing
St Thomas' Hospital
London, SE1 7EH
United Kingdom,
Email: oliver.lyons@cdhb.health.nz, alberto.smith@kcl.ac.uk Tel: +44(0)2071880214

Word count: 10 044 including abstract, references and main figure legends.

Subject terms Vascular Disease, Animal Models of Human Disease, Basic Science Research, Developmental Biology, Vascular Biology, Genetically Altered and Transgenic Models, Ultrasound

Abstract:

Venous valve (VV) failure causes chronic venous insufficiency, but the molecular regulation of valve development is poorly understood. A primary lymphatic anomaly, caused by mutations in the receptor tyrosine kinase *EPHB4,* was recently described, with these patients also presenting with venous insufficiency. Whether the venous anomalies are the result of an effect on VVs is not known. VV formation requires complex 'organization' of valve-forming endothelial cells, including their reorientation perpendicular to the direction of blood flow. Using quantitative ultrasound we identified substantial VV aplasia and deep venous reflux in patients with mutations in *EPHB4*. We used a GFP reporter, in mice, to study expression of its ligand, ephrinB2, and analysed developmental phenotypes following conditional deletion of floxed *Ephb4* and *Efnb2* alleles. EphB4 and ephrinB2 expression patterns were dynamically regulated around organizing valve-forming cells. *Efnb2* deletion disrupted the normal endothelial expression patterns of the gap junction proteins connexin37 and connexin43 (both required for normal valve development) around reorientating valve-forming cells, and produced deficient valve-forming cell elongation, reorientation, polarity, and proliferation. *Ephb4* was also required for valve-forming cell organization, and subsequent growth of the valve leaflets. These results uncover a potentially novel cause of primary human VV aplasia.

Keywords: Venous valve / reflux / primary aplasia / chronic venous insufficiency

Introduction

Unidirectional blood flow requires functional venous valves (**VV**s) which are widely distributed throughout human veins and venules, predominantly in vessels less than 100μm in diameter.(1) Lower limb VVs are typically bicuspid and situated just upstream of the confluence with a tributary.(1, 2) Failure of these valves is the central feature of the venous reflux that is seen in up to 40% of adults,(3, 4) while congenital venous valve aplasia has also been identified.(5-8) In the lower limbs, venous reflux causes chronic venous hypertension, leading to pain, oedema, hyperpigmentation, skin damage, and chronic intractable ulceration.(3, 9, 10) Our understanding of the molecular mechanisms of VV embryological development, maintenance after formation, and failure in disease is limited, and there are few therapeutic options to treat VV dysfunction.(3, 11-16) Elucidating these mechanisms and understanding how their dysfunction may lead to VV failure could facilitate the development of novel therapies.

Clinical studies have suggested a link between venous reflux and some primary lymphedemas, and we have previously shown striking human VV disease in patients with primary lymphedema caused by mutations in *FOXC2* (MIM 602402) and *GJC2* (MIM 608803*)*.(11, 17-20) Other human genetics studies have shown that mutations in the gene encoding the tyrosine kinase receptor EPHB4 (*EPHB4,* MIM 618196)*,* cause capillary malformation-arteriovenous malformation syndrome (CM-AVM2, including hereditary haemorrhagic telangiectasia and vein of Galen malformations, cutaneous malformations and arteriovenous malformations) and a primary lymphatic anomaly which includes clinical features such as central conduction lymphatic

anomaly, non-immune fetal hydrops, and atrial septal defects. (21-28). Patients with the primary lymphatic anomaly were also reported to present with varicose veins and early onset venous stasis.(21, 25, 28) In mice, early embryonic deletion of *Ephb4* in lymphatic endothelia leads to subcutaneous oedema and abnormal dermal and mesenteric lymphatic vasculature, whereas deletion in adult blood endothelia results in coronary abnormalities including capillary microhaemorrhages.(21, 29)

The Eph's are the largest family of mammalian receptor tyrosine kinases and bind to ephrins, their trans-cellular ligands.(30, 31) Cell-cell signaling may occur in either direction, resulting in cell and context-specific effects, and is involved in regulating many developmental processes including cell sorting and boundary formation.(32-34) In the cardiovascular system ephrinB2 is widely accepted as an arterial-specific marker, whereas EphB4 is used as a marker of venous endothelia.(35-37) EphrinB2-EphB4 signaling is essential for developmental angiogenesis, and global knockout of *Ephb4* is phenotypically similar to knockout of *Efnb2*, with both resulting in vascular remodeling defects and embryonic lethality.(35, 38-40) Constitutive overexpression of ephrinB2 leads to defects including abnormal intersomitic vessel patterning, aortic dissection and aneurysm formation, and early neonatal lethality due to aortic rupture.(41)

Signaling between ephrinB2 and EphB4 is required for lymphatic valve (**LV**) development and maintenance, and for formation of valves at lymphovenous junctions at the base of the neck.(12, 21, 42) LV cells fail to take on normal morphology in *Efnb2*$^{\Delta V/\Delta V}$ mice (lacking the C-terminal PDZ interaction site), and it was suggested that ephrinB2-EphB4 signaling is required to guide endothelial cell

(**EC**) migration and elongation during LV morphogenesis.(42) Blocking the forward signaling activity of EphB4 results in failure of LV formation.(43, 44) Defects in cardiac valve (**CV**) development leading to early perinatal death are found in *Efnb2*$^{\beta gal/\beta gal}$ mice, in which the cytoplasmic tail of ephrinB2 is replaced with βgal.(45) In both LV and CV, the morphological effects of loss (or inhibition) of ephrinB2-EphB4 signaling on Prox1^{hi} valve-forming cells (**VFC**s) remain unclear. Ephrin-Eph interactions result in rapid changes in cellular direction and motility, leading to boundary formation within initially mixed populations of cells (for example, in mesenchymal cells), and can inhibit communication via gap junctions across these boundaries.(31, 32, 46) In vitro, ephrinB2-EphB4 signaling controls EC repulsion and segregation, leading to clustering of EphB4- or ephrinB2-expressing cells, akin to in vivo boundary formation, but to the best of our knowledge this behaviour has not been observed in ECs in vivo.(47)

We previously showed that ephrinB2 is required for postnatal VV leaflet development and maintenance, but the expression of ephrinB2 and EphB4, and any roles in the early organization of VFCs, have not been examined.(11, 12) In this study, we show that mutations in *EPHB4* cause striking human VV disease, with an almost complete loss of VVs seen in some patients. Given the known roles for ephrin-Eph interactions in boundary formation in other tissues, we hypothesised that ephrin-Eph interactions could regulate early organizational events in VV formation. We have therefore focused on their respective roles in the regulation of the complex series of events during early valve formation in mice, which includes the organization of a set of Prox1^{hi} VFCs to form a ring of cells within the three-dimensional lumen of the vessel (stage 1 of development).(11, 12) At P0 this structure is found predominantly on the

anterior vein wall, and then extends posteriorly.(11) Using a GFP reporter we identified *Efnb2* expression within veins at the site of VV formation, and that the organization of VFCs occurs at a striking boundary between venous ECs that express ephrinB2 and those that do not. A conditional loss-of-function genetic approach has enabled us to show that both ephrinB2 and EphB4 are required for these early organizational events and that EphB4 is required for postnatal VV development.

Results

Patients with mutations in EPHB4 have fewer VVs and show deep venous reflux

Pathogenic mutations in *EPHB4* were recently described in two families with primary lymphatic related fetal hydrops (LRFH), with autosomal dominant inheritance.(21) Adults in both families had a notably early onset of lower limb venous disease. We therefore characterised the numbers of valves per vein in these patients (N=5) and an unaffected relative using ultrasonography, and compared these results to a control population (N=12, Supplementary Table 1). VVs were readily detected in the unaffected relative and other controls, but fewer VVs were detected in patients carrying a heterozygous mutation in *EPHB4,* including three patients with a mosaic mutation in *EPHB4* (fold change 0.2 ±SD 0.29 for mosaic carriers, and 0.17±0.36 for constitutive carriers, $P=1.7x10^{-11}$, ANOVA: F=30.3, 2df, Figure 1A,B, and Supplementary Figure 1). 92 veins were analysed in 13 controls, and 40 veins were analysed in 5 mosaic or constitutive *EPHB4* mutation carriers. Given the substantial loss of VVs in those with constitutive *EPHB4* mutations, too few VVs were available for detailed analysis of leaflet length in constitutive mutation carriers, but those VVs that were identified were not significantly shorter than controls (Supplementary Figure 1, fold change 1.15±0.63 for mosaic carriers, and 0.67±0.48 for constitutive carriers, P= not significant). Groups were matched for age and sex (P= not significant). Those carrying an *EPHB4* mutation had a mean popliteal reflux duration of 1.37s, above the accepted diagnostic threshold of 1s for severe deep venous reflux. Both patients with constitutive *EPHB4* mutations exhibited a mean popliteal vein reflux duration ≥1s (Figure 1C,D, Supplementary Figure 1).

EphB4 is expressed at E18 and P0 and is required for normal VFC organization

EphB4 is the main ephrinB2 receptor in the vasculature, and these proteins often exhibit a complementary expression pattern during tissue segmentation.(13, 35) Our analysis initially focused on embryonic day 18 (E18) and postnatal day 0 (P0). We localised EphB4 expression in the region of the developing valve in *Efnb2*^{GFP} mice, and then examined whether EphB4 is required for organization of VFCs at P0.

At E18, when VFCs are in the process of organizing themselves at the site of developing valves, EphB4 expression appeared to be stronger immediately upstream of areas showing VFC organization, and adjacent to VFCs with high *Efnb2* expression (Figure 2A, Supplementary Figure 2C). Quantification of *Efnb2*^{GFP} signal and EphB4 immunosignal across these organizing areas (yellow box in Figure 2A) confirmed relatively complementary expression with significantly higher EphB4 upstream and higher *Efnb2*^{GFP} downstream of the VFCs (Figure 2B). Conversely, VFCs nearer the superior or inferior edges of the vessel already coexpressed *Efnb2*^{GFP} and EphB4 (arrowheads in Figure 2A).

By P0, VFCs consistently reorientate and elongate to form a line of cells across the anterior femoral vein wall, and partly extend across the posterior wall, defined as stage 1 of VV development (schematic in Figure 2A). Prior to this, development is described as stage 0. We had thought that EphB4 expression would be complementary to *Efnb2* expression at P0, but EphB4 was immunolocalised variably throughout the valve region, with stronger expression within clusters of VFCs at the superior and inferior regions of the valve (Figure 2C, arrowheads), where we

previously identified multiple proliferating VFCs.(11) Co-expression of Ephb4 and *Efnb2* was confirmed in *Efnb2*^{GFP} mice (Figure 2D and Supplementary Figure 2B). Deletion of *Ephb4* at E15 resulted in disorganized VFCs at P0 (Figure 3A) albeit some VVs developed normally to stage 1 (Figure 3B).

Ephb4 is required for leaflet development to P6

We next localised the expression of EphB4 in VV leaflets at P6 and in adult mice. We then examined whether EphB4 is required for maturation of the valve leaflets up to P6.

EphB4 continued to be expressed in the endothelia of veins and VV leaflets at P6 and in adults (Figure 3C, left panel). Expression was strongest on the lumen surface of the valve leaflet, including cells at the free edge of valve leaflet (Figure 3C, right panel). This expression is complementary to the previously identified lack of expression of *Efnb2* in these free edge cells.(12) This could contribute to maintenance of their phenotype, which is clearly different to the rounded morphology of endothelia lining the sinus or lumen leaflet surfaces.(12)

At P6 VVs are normally at stages 3 or 4 (schematic in Figure 3), which were defined, as previously, by the presence of one or two commissures.(11) Deletion of *Ephb4* at P0 led to a complete failure of valve leaflet formation by P6, with only a few Prox1- or Foxc2-expressing cells remaining (Figure 3D,E). This phenotype (*Ephb4* deletion at P0, analysed at P6) was more consistent and severe than deletion at E15, analysed at P0 (Figure 3A).

Similarly to other gene-deletion studies resulting in loss of VFCs by P6, there was an associated failure to establish a local reduction in the density of smooth muscle cells (SMCs) around the valve (Figure 3D).(11)

VFC organization occurs at a developing boundary between ECs expressing and not expressing Efnb2

To visualise the *Efnb2* expression pattern during VFC organization we visualised the site of VV formation in the proximal femoral vein using confocal microscopy of wholemount samples from *Efnb2*^{GFP} reporter mice (Figure 4A). *Efnb2*^{GFP} signal was strong in femoral artery ECs (Figure 4A, FA), and generally absent or at very low levels in venous endothelia in all samples analysed, similar to previously reported findings.(36, 37) Expression of *Efnb2* by venous smooth muscle α-actin-expressing mural cells was not detected (data not shown). Global heterozygous knockout of *Efnb2* (in the *Efnb2*^{GFP} reporter) did not prevent development of stage 1 VVs by P0 (P = NS vs wildtype littermates, N=32 *Efnb2*$^{GFP/wt}$ VVs analysed). At E18 the patterning of Prox1^{hi} VFCs within the valve-forming region was more variable than at P0, with areas of Prox1^{hi} cells (e.g. the superior but not inferior area) showing organization (i.e. reorientation and elongation of cells, Figure 4A, upper panel vs lower panel). The organizing VFCs, and endothelia just downstream of organizing VFCs, expressed *Efnb2* (Figure 4A, green box), whilst areas without VFC organization did not develop a boundary in ephrinB2 expression (Figure 4B, blue box). Quantification of the *Efnb2*^{GFP} signal at E18 confirmed a boundary in

255 expression of *Efnb2* in regions of organized cells, but not in adjacent non-organized
256 regions (Figure 4B).
257
258 At P0 *Efnb2* was consistently expressed (and more strongly than at E18) by the line
259 of Prox1^{hi} VFCs and in cells downstream, but not upstream, of the VFCs (Figure 4A,
260 lower panel). Quantification confirmed the boundary in *Efnb2*^{GFP} signal, with a peak
261 in *Efnb2* expression coinciding with Prox1^{hi} VFCs (Figure 4C). Whilst at E18 the
262 downstream *Efnb2*^{GFP} signal was marginally higher than the upstream signal (Figure
263 4A,B), by P0 this difference was more marked (Figure 4A,C). These results suggest
264 that the *Efnb2* expression boundary is formed concomitantly with the organization of
265 Prox1^{hi} VFCs, and suggest that an Eph-ephrin interaction within venous endothelia
266 might participate in the regulation of VFC organization.
267
268 Analysis of this valve-forming region at P0 in wildtype mice by transmission electron
269 microscopy (TEM) demonstrated that development of the core of the valve leaflet is
270 more advanced than previously characterised, with the presence of interstitial cells
271 within the leaflet, which is already protruding from the vessel wall (Figure 4D, upper
272 panel).(11) VFCs at the leading edge of the protruding leaflet were partly detached
273 from the underlying basement membrane, consistent with their progressive
274 reorientation and migration (Figure 4D, upper panel, arrowheads), as has previously
275 been identified in developing LV.(48) TEM analysis at P6 and in adult mice confirmed
276 the presence of interstitial cells in murine VV (Figure 4D, middle and lower panels,
277 Supplementary Figure 3A-C), consistent with their known presence in, for example,
278 rabbit VV.(2) The presence of interstitial cells in human VV was confirmed by TEM
279 and histology (Supplementary Figure 3D,E). Connexin43 and Connexin47, proteins

implicated in human VV disease,(11) were immunolocalised to human VV interstitial cells (Supplementary Figure 3F).

Efnb2 is required for normal VFC organization

Having established the expression pattern of *Efnb2* during VFC organization, we then examined whether *Efnb2* is required for the organization of VFCs at P0. We performed conditional gene deletion using floxed *Efnb2* alleles and *Prox1Cre^{ERT2},* and quantified each valve according to developmental stage and also quantified the elongation and reorientation of Prox1^{hi} cells (as previously described).(11, 12, 48) Heterozygous deletion at E15 did not significantly affect VV development to stage 1 (Figure 5A middle panel, and B). There was, however, a small but significant reduction in VFC nuclear elongation (Figure 5C,D), but no difference in their reorientation (Figure 5E,F). Homozygous deletion of *Efnb2* resulted in disorganized VFCs that failed to reach stage 1 of development at P0, with a similar pattern of disorganization to that seen with deletion of *Ephb4* ($P<0.001$, Figure 5A lower panel, and B). Prox1^{hi} cells were present but appeared to be distributed across a wider upstream-downstream region of the vessel, and exhibited markedly reduced elongation (Figure 5C,D, $P<0.00005$) and reorientation ($P<0.005$, Figure 5E-F). These findings demonstrate that endothelial *Efnb2* is required for the normal organized patterning of VFCs at P0.

These results, together with those we described for *Ephb4*, show that the expression of EphB4 and *Efnb2* is dynamic during VV organization, and complementary expression (*Efnb2* higher downstream, EphB4 higher upstream) occurs during the process of organization at E18, but by P0 VFCs express both *Efnb2* and EphB4.

Efnb2 is required for projection of VFCs into the vessel lumen, normal expression of integrin-α9, and normal polarity

We prepared longitudinal semi-thin sections in the XZ-plane of the wholemount preparations, to more clearly examine projection of VFCs into the vessel lumen. Compared with littermate controls VFCs failed to project into the vessel lumen in homozygous *Efnb2*-deleted cells (Figure 6A,B). We hypothesised that failure to correctly express integrin-α9 could be a mechanism underlying the failure of VFCs to organize and project into the lumen in *Efnb2*-deleted mice, as integrin-α9 is required in valve formation for extracellular matrix remodeling, and for VV leaflet growth and maintenance.(11, 12, 49) At P0 integrin-α9 expression was largely localised to the line of VFCs on the anterior vein wall (Figure 6C, upper panel). After *Efnb2* deletion, the integrin-α9 expression pattern followed the abnormal, broader distribution of the Prox1^{hi} cells, and appeared haphazard (Figure 6C), likely precluding normal matrix remodeling.

Because VFCs appeared in a broader region after *Efnb2* deletion, we hypothesised that without guidance from ephrin-Eph interactions at E18 these cells would be disorientated at P0. In LV formation, lymphatic ECs elongate and migrate centrally from the edges of the vessel (48, 50) and in migratory ECs, the Golgi apparatus is positioned apically of the nucleus.(51) We therefore analysed VFC alignment by co-staining for a Golgi marker, and examined the alignment of cells with the forming VV structure (Figure 6D, upper panel). In littermate controls at P0, cells were consistently

aligned across the vessel anterior wall, whilst in all samples with homozygous *Efnb2* deletion there was a disrupted pattern (Figure 6D, lower panel).

Gap junction intercellular communication and proliferation

Expression of ephrinB's may regulate cell behaviour by modulating connexin communication domains, including via Connexin43 (Cx43).(32, 46) Cx43 and Connexin37 (Cx37) have highly regulated expression patterns around VFCs at P0, and both are required for venous, lymphatic, and lymphovenous valve formation.(11, 13, 14, 52-54) Large gap junction plaques containing Cx37 are normally expressed by Prox1^{hi} VFCs at P0, whilst Cx43 is primarily expressed in a region just upstream of the organized VFCs at P0. Homozygous deletion of Cx43 (using Prox1Cre^{ERT2}), or homozygous knockout of Cx37, results in a failure of organization of VFCs at P0, which is reminiscent of the phenotype seen with homozygous deletion of *Efnb2*.(11, 13, 14) This failure of organization at P0 is followed by complete loss of valve structure.(13) We therefore examined the expression patterns of Cx37 and Cx43 relative to *Efnb2* expression in the *Efnb2^{GFP}* reporter mice, and after homozygous deletion of *Efnb2.* The normally highly restricted expression patterns of Cx37 and Cx43 were disrupted at P0 following homozygous *Efnb2* deletion (Figure 7A,B). In the *Efnb2^{GFP}* reporter, Cx37 localisation indicated gap junction plaque formation around *Efnb2*-expressing VFCs (Figure 7A, white arrowheads in upper panel), whilst after *Efnb2* deletion, no plaque formation was identified (or possibly plaques were very much smaller), and Cx37 expression appeared more widespread in the region of the VFCs (Figure 7B).

In previous genetic loss-of-function experiments (including knockout of Cx37), disruption of VFC organization was associated with a reduction in VFC

proliferation,(11) and so we next examined whether deletion of *Efnb2* altered VFC proliferation or apoptosis. As previously, Ki67-positive proliferating VFCs appeared more abundant in the superior & inferior regions of the valve at P0.(11) A reduction in the proportion of proliferating VFCs was seen following *Efnb2* deletion ($P<0.001$, Figure 7C,D), but no effect on apoptosis (as detected by Caspase-3 expression) was observed (data not shown).

Discussion

We have identified human venous valve failure and deep venous reflux caused by mutations in *EPHB4*. This phenotype was more severe (i.e. a greater loss of valves) than that previously identified in patients with mutations in *FOXC2* or *GJC2* (a fold change vs controls of 0.2 ±SD 0.29 (mosaic *EPHB4*) or 0.17 ±0.36 (constitutive heterozygous *EPHB4*) for the reduction in mean VVs per vein).(11) Almost all of these patients did not have clinical evidence of chronic lower limb primary lymphedema. Some presented with non-immune foetal hydrops, which was of lymphatic origin, but it had resolved soon after birth. Following that, their most obvious clinical sign of disease was early onset prominent or varicose veins, and venous insufficiency.(21) We now know that this is venous valvular aplasia, and therefore mutations in *EPHB4* should be considered as a cause of primary venous valvular aplasia.(5-8, 21, 55) Dysfunction of the deep venous valves increases the rate of progression of chronic venous insufficiency, with a higher rate of chronic venous ulcer formation. The management of deep venous reflux is extremely challenging, as currently there are no reliably effective therapies beyond invasive surgical construction of neovalves.(3)

Heterozygous mutations in *EPHB4* are reported to cause CM-AVM2, vein of Galen aneurysmal malformation, Lymphatic Related Foetal Hydrops (LRFH), and central conducting lymphatic anomaly (CCLA), but the mechanism(s) underlying these different presentations remain unclear.(21, 22, 25, 26, 28) The clinical descriptions of patients with a lymphatic phenotype such as LRFH and CCLA also include clear features of venous disease such as varicose veins, venous hypertension or venous

386 reflux. Similar to the cases presented, it seems likely that the patients reported by Li
387 *et al* may also be affected by VV aplasia and deep venous reflux (considering their
388 increased lower limb pigmentation and venous stasis).(25) The early age at onset of
389 clinical signs of venous insufficiency (for example varicose veins, hemosiderin
390 deposition) in affected individuals, and the near absence of VVs in the scanned veins
391 of affected children observed here, is consistent with a failure of VV formation, rather
392 than early degeneration. These features are not described for CM-AVM2, or vein of
393 Galen aneurysmal malformation, and it is unclear whether the mutations causing
394 these syndromes will also cause VV defects.(22, 26) EphrinB2 is required for normal
395 cardiac valve (CV) formation in mice, but no CV defects were noted on
396 echocardiography in the patients reported here, or those reported elsewhere.(21, 25,
397 28) It remains unclear how, in the settings of developmental blood vessel formation
398 and in the adult capillary bed, ephrinB2-EphB4 interaction leads to specification and
399 subsequent maintenance of arterial and venous endothelia, yet both are expressed in
400 mature veins to regulate the formation of valves.(12, 22, 23, 38, 41) Further work is
401 needed to delineate the context and maturation-dependent regulation of these
402 endothelia.
403
404 Previous *in-vitro* analysis of the *EPHB4* mutations studied here (p.Arg739Glu and
405 p.Ile782Ser) demonstrated that they exhibit greatly reduced kinase activity, but do
406 not exert a dominant negative effect on the expression of wildtype EPHB4
407 protein.(21) Any effect on wildtype EPHB4 activity is unknown. The ratio of ephrinB2
408 to EphB4 expression is disturbed at both mRNA and protein level in ECs cultured
409 from patient arterio-venous malformations, with greatly reduced EphB4 expression
410 compared to a control cell line.(56) The mutant EPHB4 protein implicated in CM-

AVM2 becomes trapped in vesicles (22, 28), whilst that implicated in LRFH is presented on the cell membrane (28), but the exact signalling implications of these findings are yet to be elucidated. The requirement for ephrin-Eph signalling at multiple stages of VV development and maintenance complicates any attempt to develop molecular therapy aiming to directly restore valve function. It is possible that pharmacological stimulation or inhibition of the pathway downstream of EPHB4 might be helpful to overcome the resulting aberrant signalling.(22, 25)

The extent of overlap of the genetic causes of venous valve failure and varicose veins is unclear since regulation of VVs is understudied, but some important indications of similarity have already emerged, including the identification of *PPP3R1* and *PIEZO1* in genome wide association studies of varicose veins, and in mice as critical regulators of VV development.(11, 57, 58) Delineating the roles of the various genes implicated in VV pathogenesis is important and may lead to novel therapies, which could be targeted towards patients at risk of deterioration to chronic ulceration.(59)

In this study we have identified a striking 'boundary' in the endothelial expression of *Efnb2* at the site of developing VVs (meaning a demarcation between ephrinB2^{lo} upstream cells and ephrinB2^{hi} VFCs and cells immediately downstream), and that both ephrinB2 and EphB4 are required for normal organization of VFCs at this critical stage of development in mice. Since ephrinB2 remains the only known ligand for EphB4, this leads us to speculate that an ephrinB2-EphB4 interaction within venous endothelia regulates VV formation. We also show that EphB4 is required for VV maturation. At E18, in areas where VFCs appeared to be in the process of

reorientating to become transversely aligned, EphB4 expression was stronger just upstream of the ephrinB2-expressing VFCs. We speculate that at this time point, EphB4^{hi} regions upstream from VFCs may be acting to repel ephrinB2^{hi} VFCs, guiding them to reorientate to lie transversely across the vessel to form a line across the anterior of the lumen. We were unable to localise ephrinB2 because of a lack of specific antibodies, and this inability to colocalise EphB4 and ephrinB2 is a limitation of our study. In wildtype littermates VFC polarity was aligned with the boundary and developing ring of VFCs, whilst after *Efnb2* deletion VFC polarity was disorganized and cells were spread over a wider upstream-downstream region. These results are consistent with previous *in-vitro* findings, showing that ephrinB2-EphB4 interaction leads to separation and clustering of initially mixed populations of EphB4- and ephrinB2-expressing ECs.(47) *In-vitro,* treatment with ephrinB2-Fc stimulates migration of HUVECS, and it is possible that ephrinB2 promotes the migration of VFCs.(60)

It remains unknown how *Efnb2* expression within veins is regulated. We have shown that the *Efnb2* boundary forms as the VFCs organize, and it may be regulated by the VFCs themselves as they organize. Notably, BMP9 controls lymphatic remodeling and LV formation, and also induces *Efnb2* expression in lymphatic and blood endothelia in vitro, but it is not known whether there is a VV phenotype in *Bmp9*$^{-/-}$ mice.(61, 62) The extent to which there is proliferation of VFCs between E18 and P0, or whether there is de-novo differentiation of new Prox1^{hi} cells from surrounding endothelium, remains unclear.

Normal blood flow is required for postnatal VV maturation (11) and *Efnb2*-dependent protrusion of cells into the lumen at P0 could expose VFCs to higher fluid shear forces, particularly as the vessel lumen becomes more acutely narrowed (e.g. at stage 2 of VV development).(12) Shear-regulated signaling might co-ordinate subsequent events in VV formation, for example commissure formation. In embryonic stem cell derived ECs in vitro, *Efnb2* is upregulated by shear stress, which may contribute to the stimulation of VV leaflet growth post-natally.(12, 63) This notion is consistent with the role of the oscillatory shear stress/Gata2/Foxc2 axis in LV endothelial differentiation, and the potential role of wall shear stress gradients in demarcating the locations of valve formation upstream of tributaries.(64-66) Deletion of the mechanosensory ion channel *Piezo1* results in defective VVs at P3, again consistent with a role for fluid shear in patterning VV (in addition to LV) formation.(57, 67)

Signaling downstream of ephrin-Eph interactions can, for example, inhibit gap junction formation at the boundary between two cell populations, likely by cell repulsion preventing stable contacts between cells.(32) It seems likely that cell-cell repulsion between ephrinB2^{hi} VFCs and EphB4^{hi};ephrinB2^{lo} upstream cells at E18 patterns the migration of VFCs. It is unknown whether gap-junction signalling is important in this process, but loss of either Cx37 or Cx43 in mice leads to a similar phenotype with failure of VFC organization.(11) Homozygous *Efnb2* deletion disrupted the normally highly restricted expression patterns of Cx37 and Cx43 at P0, suggesting that gap junctional communication is disrupted. Gap junction plaque size varies depending on how many channels are clustered in the plaque. It is possible that plaques were present but much smaller, although this would also be expected to

485 reduce cell-cell communication.(68) We were unfortunately unable to develop
486 experiments to demonstrate gap junctional VFC cell-cell communication in vivo, or
487 confirm how this may be disrupted after deletion of *Ephb4* or *Efnb2*.
488
489 Mutations in *EFNB1* cause craniofrontonasal syndrome, whilst mice heterozygous for
490 *Efnb1* display skull defects that are thought to be mediated by inhibition of normal
491 gap-junctional communication via Cx43 at ectopic ephrin-Eph boundaries. EphrinB1
492 directly interacts with Cx43 and regulates its cellular distribution, and disruption of
493 gap junction plaques was seen in *Efnb1*$^{+/-}$ mice.(46) Whilst deletion of *Efnb2* resulted
494 in loss of large Cx37 plaques in VFCs, any direct interaction between ephrinB2 and
495 Cx37 remains to be determined. Although not directly demonstrated in our
496 experiments, it is reasonable to assume that following *Efnb2* deletion, as the Prox1^{hi}
497 VFCs are further apart and are physically separated, there will be less
498 communication between these cells via gap junctions (e.g. incorporating Cx37).
499 EphrinB2 organizes VFC positioning and therefore facilitates the formation of
500 functional gap junctions between adjacent VFCs. It is plausible, therefore, that
501 disruption of connexin expression patterning and gap junctional communication may
502 be part of the mechanism that underlies the phenotype seen following *Efnb2*
503 deletion.(46)
504
505 In wildtype mice at P0 Cx43 was expressed upstream of the developing VV and was
506 not clearly expressed by the Prox1^{hi} VFCs that express ephrinB2.(11) Cx43 is clearly
507 expressed by cells that also express EphB4. With deletion of *Efnb2,* Cx43 expression
508 appeared more dispersed throughout the femoral vein, suggesting ephrinB2 is
509 required for the restriction of the Cx43 expression domain. In cardiomyocytes, EphB4

510 physically associates with Cx43, and EphB activation inhibited cardiomyocyte gap
511 junctional electrical coupling.(69) It is possible that in upstream endothelia, signaling
512 through EphB4 could inhibit gap junction communication via Cx43.
513
514 It is unclear why the VV phenotype following *Ephb4* deletion was slightly weaker than
515 that in *Efnb2* deleted mice. EphrinB2 is more promiscuous, binding to EphB4, EphB3
516 and EphB2, while EphB4 exclusively interacts with ephrinB2.(38, 70) Isolated
517 knockout of either *Ephb2* or *Ephb3* does not induce any cardiovascular phenotype,
518 but a third of double knockouts have severely defective angiogenesis that resembles
519 much of the phenotype of *Efnb2*$^{-/-}$ mice.(38) EphB3 expression has been reported in
520 veins (while EphB2 is expressed in nonvascular mesenchymal cells), but we could
521 not detect specific signals for EphB2 or EphB3 in veins by immunohistology (data not
522 shown). EphrinB2 regulates cell morphology and motility independently of binding its
523 receptors in vitro, which could partly explain the stronger phenotype seen with *Efnb2*
524 deletion.(71) In sprouting angiogenesis, ephrinB2 is required for endocytosis and
525 signalling of other important regulators of EC function including Vegfr2 and Vegfr3
526 (which are expressed in developing VVs), and could play similar roles in VFC
527 organization.(12, 39, 40) The slight difference in the phenotypes following deletion
528 of *Efnb2* and *Ephb4* could be caused by differences in their protein stability, which
529 we were unable to investigate, in part because of the lack of specific antibodies
530 raised against ephrinB2. We could not confirm reduced *Ephb4* or *Efnb2* mRNA levels
531 following conditional gene deletion, due to our inability to specifically isolate venous
532 valve cells, but this has been confirmed for *Efnb2* deletion in lymphatic
533 endothelium.(72)
534

Detachment of VFCs from their underlying basement membrane has previously been identified in LV formation, during angiogenesis, and we now show it here in VV formation.(48, 73) Due to detachment, cell-cell contacts are highly restricted, and this is likely to impact cell-cell signalling processes.(48, 74) In vitro, soluble ephrinB2-Fc acts anti-adhesively, and the high ephrinB2 expression in VFCs could promote their detachment from the underlying basement membrane to facilitate reorientation and organization.(47)

We have previously analysed VFC nuclear reorientation and elongation in wholemount confocal microscopy to characterise phenotypes at P0 / stage 1 of VV development.(11) Here, we show that VFCs not only protrude into the vessel lumen at this stage, but that this protrusion is abolished following homozygous *Efnb2* deletion. We also identify that ingress of interstitial cells is already occurring at this early stage and confirm their persistence in P6 and adult murine VV, and in adult human VV. Their existence has previously been demonstrated in human, rat and rabbit VV, in contrast to LV, which lack interstitial cells.(2, 49, 54) In lymphovenous valve development, mural cells are recruited into the valve leaflets during maturation, but the developmental origin of these cells in VVs is currently unknown.(54) The identity, origin and functions of these cells in VVs will be the subject of future studies.

Our data showing that EphB4 is required for post-natal development is consistent with the phenotype resulting from *Efnb2* deletion at P2 or P0.(11, 12) Almost all Prox1^{hi} and Foxc2^{hi} VFCs were absent at P6, in contrast to deletion of *Ppp3r1* (CnB1) in which a clear ring of Prox1 and Foxc2-expressing cells remains.(11) This is consistent with a requirement for EphB4 (and ephrinB2) to develop/maintain the

phenotype of free-edge cells to P6, rather than just growth of VV leaflets.(11) The failure to establish a local reduction in the density of smooth muscle cells (SMCs) around the VV at P6 after *Ephb4* deletion at P0 is consistent with the endothelial VFC-to-SMC signaling that controls this reduction in SMC density around LVs.(31, 75-77)

Conclusions

In addition to an increased risk of lymphatic-related foetal hydrops, we have shown that patients carrying heterozygous mutations in *EPHB4* have very few VVs, with early onset deep venous reflux indicating that the observed venous insufficiency is due to venous valve aplasia. By studying mice, it was demonstrated that ephrinB2 and EphB4 pattern the organization of valve-forming cells at P0, and are required for cellular reorientation, elongation, protrusion and proliferation, adding to our understanding of the complex venous valve developmental programme. Postnatal deletion of *Ephb4* leads to complete loss of the valve, which could explain the phenotype observed in the patients.

Methods

Human VV ultrasonography

The brachial, basilic, popliteal, and short saphenous veins underwent ultrasonographic evaluation in London (Phillips IU22 with L17-5MHz/L9-3MHz probes) and VV maximum leaflet measurements obtained offline (Xcelera Cath Lab software, Phillips). Reproducibility was determined previously.(11) For each vein, the number of VVs and VV length was normalised to the mean value in the respective control veins from our existing control population, and additional new controls, and the mean number of VVs per vein, per patient, was compared. Deep venous (popliteal) reflux duration was measured bilaterally after distal manual compression whilst standing, and the mean taken, with reflux defined as ≥0.5s, and severe reflux as >1s.(78-80) Because deep venous reflux is rare, popliteal venous reflux was not routinely measured in the entire control population, but was subsequently measured in additional controls.(81) Genotyping was performed at St George's, University of London and in Bergen.(21)

Mouse lines

Wildtype analyses were carried out in BALB/C mice obtained from Charles River UK. *Prox1CreER*^{T2} (12), Rosa26^{mTmG} (82), *Efnb2*^{lx} (83), and *Efnb2*^{GFP} (84) mice have been described previously and were maintained on C57BL/6 backgrounds. Tamoxifen/4OH-Tamoxifen (in peanut or sunflower oil, Sigma) was injected i.p. either 1mg at E15 for analysis at P0, or 50µg at P0 for analysis at P6 in order to induce Cre activity in *Prox1CreER*^{T2} mice.(12) To delay labour 37.5µg/g.Ms weight progesterone was given i.p. at E15+E18 and embryos analysed at 'E19', equivalent to P0. We

compared VV in *Prox1CreER^{T2}*+ with *Prox1CreER^{T2}*- littermate controls in all deletion experiments.

Electron microscopy

Mice were culled and perfused via the aorta with heparinised PBS (hPBS, 25mg/L, MP Biomedicals) prior to fixation overnight in glutaraldehyde (2.5% v/v in 0.1M cacodylate buffer, pH 7.4, 4^{o}C) and post-fixation in osmium tetroxide (1% w/v in 0.1M cacodylate, pH 7.4, 4^{o}C) for 1.5hrs. All samples were dehydrated through graded ethanols, equilibrated with propylene oxide, infiltrated with epoxy resin (TAAB) and polymerised at 70^{o}C for 24hrs. Semithin sections (0.45µm) were cut and stained with 1% Toluidine Blue. For analysis of protruding VFCs, >90 serial semithin sections were analysed per sample (unpaired t test). For 3D reconstructions at P0, semi-thin sections (0.45µm) were photographed (Leitz DMRB microscope, Micropublisher 3.3RTV camera), aligned in ImageJ (NIH) and reconstructed using Amira (Thermo Fisher Scientific). Ultrathin sections (50-70nm, Reichert-Jung ultramicrotome) were mounted and contrasted using uranyl acetate/lead citrate for examination (Hitachi H7600, 80kV, AMT digital camera).(85) For quantification of interstitial cells at P6, the length of the leaflet was measured in ImageJ, and the number of whole interstitial cell nuclei counted. Human great saphenous veins (obtained during coronary artery bypass grafting) were opened prior to processing as per murine samples, with visualisation of ultrathin sections using a Hitachi S-3500N microscope.

Immunohistochemistry

Mice were culled and perfusion fixed via the aorta and femoral vein by perfusion with hPBS followed by 4% formaldehyde, and then further fixed for 24hrs. The external

iliac and femoral veins were excised, embedded in wax, and 5μm sections were incubated with primary antibody and washed prior to amplification using polymer horseradish peroxidase (Menarini) and signal detection using SG peroxidase substrate (Vector). Sections were photographed using a Micropublisher 3.3RTV camera mounted on a Leitz DMRB microscope with PL Fluotar ×20 lens (Leica).

Wholemount immunostaining and analysis

Mice were culled and perfused with hPBS via the aorta prior to fixation in 4% paraformaldehyde (PFA) followed by blocking in 3%v/v donkey serum, 0.3% Triton-x100 and further dissection prior to incubation with primary antibodies, and washing prior to localisation with fluorophore-conjugated secondary antibodies. Samples were finally dissected and mounted in Prolong Gold (Invitrogen). Valves were imaged using a Leica SP5 confocal microscope (1024x1024 resolution, 8-bit) to produce Z projections (NIH ImageJ) of median filtered (Leica LASAF/ImageJ, except for connexin localisation or fluorescence quantification) stacks. Lookup tables were linear. Control samples were incubated either with the appropriate non-immune IgG and then secondary antibody, or streptavidin-conjugated fluorophore alone (Supplementary Figure 2A).

For analysis of VFC organization, $Prox1^{hi}$ nuclear elongation (proportion with length:width ratio ≥2) and reorientation (proportion with long axis ≥40degrees from the vessel centreline, in nuclei with length:width ratio ≥2) were quantified in z-projections (NIH ImageJ) as previously described.(11, 48)

For analysis of *Efnb2*^{GFP} expression at E18-P0 (Figure 4) Z-projections of confocal z-stacks were oriented with flow left to right and the centre line of the vessel horizontal. For each valve 7-12 10x100μm regions of interest, each centred on the VFC upstream edge, were analysed (ImageJ). Mean intensity profiles for each fluorophore were converted to z-scores and the mean of 6 VVs plotted. At E18, areas with and without Prox1^{hi} organizing VFCs were analysed separately.

For analysis of areas of expression of Ephb4 and Efnb2GFP at E18 (Figure 2B) an XZ projection (13.6μm deep) across the reorientating VFCs was reconstructed (NIH ImageJ) and the relative fluorescence intensity profile for Efnb2GFP and EphB4 plotted. For quantification, for each valve 4-6 50μm linear regions of interest were drawn, centred on the VFC leading edge, at E18, for N=6 VVs. Ephb4 upstream vs downstream intensity was compared (T Test).

For analysis of cell orientation by co-immunostaining of nucleus and Golgi, stacks of 0.5μm optical sections were analysed (ImageJ) to identify the Golgi for each VFC, and an arrow drawn from nuclear centre to Golgi centre. The z-projection of all arrows is shown.

Antibodies

Antibodies: Rabbit anti- Cx43 (Cell Signaling Technology 3512), Cx37 (CX37A11, Alpha diagnostics), Prox1 (11-002P, Angiobio), ki67 (ab15580, Abcam), and Golgi apparatus protein 1 (ab103439, Abcam); sheep anti- Foxc2 (AF6989, R&D); goat anti- EphB4 (BAF446, R&D); rat anti- PECAM1 (clone MEC 13.3, BD); and mouse anti- α smooth muscle actin (clone 1A4 conjugated to Cy3, Sigma). For fluorescence

signal detection secondary antibodies or streptavidin were conjugated to Dylight-405/488/550/649 (Jackson Immunoresearch).

Statistics

For VV developmental stage 0-4 quantification, data represent the proportion of VV reaching each developmental stage. P values represent the difference in proportion of valves at each stage versus their wild-type littermates (Chi square/Fisher's Exact test as appropriate). Comparisons of VFC nuclear elongation and reorientation between groups were analysed by one-way ANOVA & Bonferroni post hoc tests. Age and sex matching for patient ultrasonography was tested respectively by two-tailed unpaired t-test and Fisher's exact test. All analyses were carried out using IBM SPSS Statistics 24, and Graphpad PRISM v8. A P value less than 0.05 was considered significant. Ultrasonographers were blinded to participant genotype during scanning, and image analysis/quantification. Experiments were not randomised.

Study approval

All human studies and animal studies were carried out in accordance with national regulations and ethical approvals in the UK and Sweden (Health Research Authority 12/LO/1164, 10/H0701/68, C130/15). Written informed consent was obtained from all participants.

Author contributions

The authors have declared that no conflict of interest exists.

All authors designed research studies, OL, JW, CS, MI, AA, MH, MF, GV conducted experiments, acquired & analysed data. PM, SJ, SB, SM, PO, provided patients; OL,

AS and TM funded this study; all authors reviewed drafts and approved the manuscript.

Acknowledgements

OL was funded by: Academy of Medical Sciences Starter Grant for Clinical Lecturers, British Heart Foundation Centre of Research Excellence Travel Grant, and the Medical Research Council.

Supplemental Data

Supplemental data includes one table and three figures.

References

1. Phillips MN, et al. Micro-venous valves in the superficial veins of the human lower limb. *Clin Anat.* 2004;17(1):55-60.

2. Gottlob R, et al. *Venous valves : morphology, function, radiology, surgery.* Wien ; New York: Springer-Verlag; 1986.

3. Eberhardt RT, and Raffetto JD. Chronic venous insufficiency. *Circulation.* 2014;130(4):333-46.

4. Labropoulos N, et al. The role of venous reflux and calf muscle pump function in nonthrombotic chronic venous insufficiency. Correlation with severity of signs and symptoms. *Arch Surg.* 1996;131(4):403-6.

5. Friedman EI, et al. Congenital venous valvular aplasia of the lower extremities. *Surgery.* 1988;103(1):24-6.

6. Gorenstein A, et al. Congenital aplasia of the deep veins of lower extremities in children: the role of ascending functional phlebography. *Surgery.* 1986;99(4):414-20.

7. Bollinger A, et al. [Valve agenesis and dysplasia of leg veins. Morphological and functional studies]. *Schweizerische medizinische Wochenschrift.* 1971;101(37):1348-53.

8. Plate G, et al. Congenital vein valve aplasia. *World J Surg.* 1986;10(6):929-34.

9. Meissner M, et al. The hemodynamics and diagnosis of venous disease. *Journal of Vascular Surgery.* 2007;46(6):S4-S24.

10. Lyons OT, et al. Redox dysregulation in the pathogenesis of chronic venous ulceration. *Free radical biology & medicine.* 2019.

11. Lyons O, et al. Human venous valve disease caused by mutations in FOXC2 and GJC2. *The Journal of experimental medicine.* 2017;214:2437-52.

12. Bazigou E, et al. Genes regulating lymphangiogenesis control venous valve formation and maintenance in mice. *J Clin Invest.* 2011;121(8):2984-92.

13. Munger SJ, et al. Absence of venous valves in mice lacking Connexin37. *Dev Biol.* 2013;373(2):338-48.

14. Munger SJ, et al. Segregated Foxc2, NFATc1 and Connexin expression at normal developing venous valves, and Connexin-specific differences in the valve phenotypes of Cx37, Cx43, and Cx47 knockout mice. *Dev Biol.* 2016;412(2):173-90.

15. Goel RR, et al. Surgery for deep venous incompetence. *The Cochrane database of systematic reviews.* 2015(2):CD001097.

16. Geng X, et al. Intraluminal valves: development, function and disease. *Disease models & mechanisms.* 2017;10(11):1273-87.

17. Connell FC, et al. The classification and diagnostic algorithm for primary lymphatic dysplasia: an update from 2010 to include molecular findings. *Clin Genet.* 2013;84(4):303-14.

18. Rosbotham JL, et al. Distichiasis-lymphoedema: clinical features, venous function and lymphoscintigraphy. *The British journal of dermatology.* 2000;142(1):148-52.

19. Mellor RH, et al. Mutations in FOXC2 Are Strongly Associated With Primary Valve Failure in Veins of the Lower Limb. *Circulation.* 2007;115(14):1912-20.

20. Ostergaard P, et al. Rapid identification of mutations in GJC2 in primary lymphoedema using whole exome sequencing combined with linkage analysis with delineation of the phenotype. *J Med Genet.* 2011;48(4):251-5.

21. Martin-Almedina S, et al. EPHB4 kinase-inactivating mutations cause autosomal dominant lymphatic-related hydrops fetalis. *J Clin Invest.* 2016;126(8):3080-8.

22. Amyere M, et al. Germline Loss-of-Function Mutations in EPHB4 Cause a Second Form of Capillary Malformation-Arteriovenous Malformation (CM-AVM2) Deregulating RAS-MAPK Signaling. *Circulation.* 2017;136(11):1037-48.

765 23. Wooderchak-Donahue WL, et al. Phenotype of CM-AVM2 caused by variants
766 in EPHB4: how much overlap with hereditary hemorrhagic telangiectasia
767 (HHT)? *Genetics in medicine : official journal of the American College of*
768 *Medical Genetics.* 2019;21(9):2007-14.

769 24. Yu J, et al. EPHB4 Mutation Implicated in Capillary Malformation-
770 Arteriovenous Malformation Syndrome: A Case Report. *Pediatric dermatology.*
771 2017;34(5):e227-e30.

772 25. Li D, et al. Pathogenic variant in EPHB4 results in central conducting
773 lymphatic anomaly. *Hum Mol Genet.* 2018;27(18):3233-45.

774 26. Vivanti A, et al. Loss of function mutations in EPHB4 are responsible for vein
775 of Galen aneurysmal malformation. *Brain : a journal of neurology.*
776 2018;141(4):979-88.

777 27. Duran D, et al. Mutations in Chromatin Modifier and Ephrin Signaling Genes in
778 Vein of Galen Malformation. *Neuron.* 2019;101(3):429-43 e4.

779 28. Martin-Almedina S, et al. Janus-faced EPHB4-associated disorders: novel
780 pathogenic variants and unreported intrafamilial overlapping phenotypes.
781 *Genetics in medicine : official journal of the American College of Medical*
782 *Genetics.* 2021.

783 29. Luxan G, et al. Endothelial EphB4 maintains vascular integrity and transport
784 function in adult heart. *eLife.* 2019;8.

785 30. Hirai H, et al. A novel putative tyrosine kinase receptor encoded by the eph
786 gene. *Science.* 1987;238(4834):1717-20.

787 31. Kania A, and Klein R. Mechanisms of ephrin-Eph signalling in development,
788 physiology and disease. *Nature reviews Molecular cell biology.*
789 2016;17(4):240-56.

790 32. Mellitzer G, et al. Eph receptors and ephrins restrict cell intermingling and
791 communication. *Nature.* 1999;400(6739):77-81.

792 33. Xu Q, et al. In vivo cell sorting in complementary segmental domains mediated
793 by Eph receptors and ephrins. *Nature.* 1999;399(6733):267-71.

794 34. Batlle E, and Wilkinson DG. Molecular mechanisms of cell segregation and
795 boundary formation in development and tumorigenesis. *Cold Spring Harbor*
796 *perspectives in biology.* 2012;4(1):a008227.

797 35. Gerety SS, et al. Symmetrical mutant phenotypes of the receptor EphB4 and
798 its specific transmembrane ligand ephrin-B2 in cardiovascular development.
799 *Mol Cell.* 1999;4(3):403-14.

800 36. Gale NW, et al. Ephrin-B2 selectively marks arterial vessels and
801 neovascularization sites in the adult, with expression in both endothelial and
802 smooth-muscle cells. *Dev Biol.* 2001;230(2):151-60.

803 37. Shin D, et al. Expression of ephrinB2 identifies a stable genetic difference
804 between arterial and venous vascular smooth muscle as well as endothelial
805 cells, and marks subsets of microvessels at sites of adult neovascularization.
806 *Dev Biol.* 2001;230(2):139-50.

807 38. Adams RH, et al. Roles of ephrinB ligands and EphB receptors in
808 cardiovascular development: demarcation of arterial/venous domains,

809 vascular morphogenesis, and sprouting angiogenesis. *Genes Dev.*
810 1999;13(3):295-306.

811 39. Wang Y, et al. Ephrin-B2 controls VEGF-induced angiogenesis and
812 lymphangiogenesis. *Nature.* 2010;465(7297):483-6.

813 40. Sawamiphak S, et al. Ephrin-B2 regulates VEGFR2 function in developmental
814 and tumour angiogenesis. *Nature.* 2010;465(7297):487-91.

815 41. Oike Y, et al. Regulation of vasculogenesis and angiogenesis by EphB/ephrin-
816 B2 signaling between endothelial cells and surrounding mesenchymal cells.
817 *Blood.* 2002;100(4):1326-33.

818 42. Makinen T. PDZ interaction site in ephrinB2 is required for the remodeling of
819 lymphatic vasculature. *Genes & Development.* 2005;19(3):397-410.

820 43. Zhang G, et al. EphB4 forward signalling regulates lymphatic valve
821 development. *Nat Commun.* 2015;6:6625.

822 44. Katsuta H, et al. EphrinB2-EphB4 signals regulate formation and maintenance
823 of funnel-shaped valves in corneal lymphatic capillaries. *Investigative*
824 *ophthalmology & visual science.* 2013;54(6):4102-8.

825 45. Cowan CA, et al. Ephrin-B2 reverse signaling is required for axon pathfinding
826 and cardiac valve formation but not early vascular development.
827 *Developmental Biology.* 2004;271(2):263-71.

828 46. Davy A, et al. Inhibition of gap junction communication at ectopic Eph/ephrin
829 boundaries underlies craniofrontonasal syndrome. *PLoS Biol.*
830 2006;4(10):e315.

831 47. Fuller T, et al. Forward EphB4 signaling in endothelial cells controls cellular
832 repulsion and segregation from ephrinB2 positive cells. *J Cell Sci.* 2003;116(Pt
833 12):2461-70.

834 48. Tatin F, et al. Planar Cell Polarity Protein Celsr1 Regulates Endothelial
835 Adherens Junctions and Directed Cell Rearrangements during Valve
836 Morphogenesis. *Dev Cell.* 2013;26(1):31-44.

837 49. Bazigou E, et al. Integrin-α9 Is Required for Fibronectin Matrix Assembly
838 during Lymphatic Valve Morphogenesis. *Developmental Cell.* 2009;17(2):175-
839 86.

840 50. Bazigou E, et al. Primary and secondary lymphatic valve development:
841 molecular, functional and mechanical insights. *Microvascular research.*
842 2014;96:38-45.

843 51. Francis R, et al. Connexin43 modulates cell polarity and directional cell
844 migration by regulating microtubule dynamics. *PLoS One.* 2011;6(10):e26379.

845 52. Kanady JD, et al. Connexin37 and Connexin43 deficiencies in mice disrupt
846 lymphatic valve development and result in lymphatic disorders including
847 lymphedema and chylothorax. *Dev Biol.* 2011;354(2):253-66.

848 53. Kanady JD, et al. Combining Foxc2 and Connexin37 deletions in mice leads to
849 severe defects in lymphatic vascular growth and remodeling. *Dev Biol.*
850 2015;405(1):33-46.

851 54. Geng X, et al. Multiple mouse models of primary lymphedema exhibit distinct
852 defects in lymphovenous valve development. *Dev Biol.* 2016;409(1):218-33.

853 55. Leu HJ. Familiar congenital absence of valves in the deep leg veins.
854 *Humangenetik.* 1974;22(4):347-9.

855 56. Fehnel KP, et al. Dysregulation of the EphrinB2-EphB4 ratio in pediatric
856 cerebral arteriovenous malformations is associated with endothelial cell
857 dysfunction in vitro and functions as a novel noninvasive biomarker in patients.
858 *Experimental & molecular medicine.* 2020;52(4):658-71.

859 57. Nonomura K, et al. Mechanically activated ion channel PIEZO1 is required for
860 lymphatic valve formation. *Proc Natl Acad Sci U S A.* 2018;115(50):12817-22.

861 58. Shadrina AS, et al. Varicose veins of lower extremities: Insights from the first
862 large-scale genetic study. *PLoS genetics.* 2019;15(4):e1008110.

863 59. Jones GT, et al. A variant of the castor zinc finger 1 (CASZ1) gene is
864 differentially associated with the clinical classification of chronic venous
865 disease. *Scientific reports.* 2019;9(1):14011.

866 60. Zheng LC, et al. Ephrin-B2/Fc promotes proliferation and migration, and
867 suppresses apoptosis in human umbilical vein endothelial cells. *Oncotarget.*
868 2017;8(25):41348-63.

869 61. Kim JH, et al. BMP9 induces EphrinB2 expression in endothelial cells through
870 an Alk1-BMPRII/ActRII-ID1/ID3-dependent pathway: implications for
871 hereditary hemorrhagic telangiectasia type II. *Angiogenesis.* 2012;15(3):497-
872 509.

873 62. Levet S, et al. Bone morphogenetic protein 9 (BMP9) controls lymphatic
874 vessel maturation and valve formation. *Blood.* 2013;122(4):598-607.

875 63. Masumura T, et al. Shear stress increases expression of the arterial
876 endothelial marker ephrinB2 in murine ES cells via the VEGF-Notch signaling
877 pathways. *Arterioscler Thromb Vasc Biol.* 2009;29(12):2125-31.

878 64. Mahamud MR, et al. GATA2 controls lymphatic endothelial cell junctional
879 integrity and lymphovenous valve morphogenesis through miR-126.
880 *Development.* 2019;146(21).

881 65. Sabine A, et al. Mechanotransduction, PROX1, and FOXC2 cooperate to
882 control connexin37 and calcineurin during lymphatic-valve formation. *Dev Cell.*
883 2012;22(2):430-45.

884 66. Michalaki E, et al. Perpendicular alignment of lymphatic endothelial cells in
885 response to spatial gradients in wall shear stress. *Communications biology.*
886 2020;3(1):57.

887 67. Choi D, et al. Piezo1 incorporates mechanical force signals into the genetic
888 program that governs lymphatic valve development and maintenance. *JCI*
889 *insight.* 2019;4(5).

890 68. Solan JL, and Lampe PD. Spatio-temporal regulation of connexin43
891 phosphorylation and gap junction dynamics. *Biochimica et biophysica acta*
892 *Biomembranes.* 2018;1860(1):83-90.

893 69. Ishii M, et al. EphB signaling inhibits gap junctional intercellular
894 communication and synchronized contraction in cultured cardiomyocytes.
895 *Basic research in cardiology.* 2011;106(6):1057-68.

70. Sakano S, et al. Characterization of a ligand for receptor protein-tyrosine kinase HTK expressed in immature hematopoietic cells. *Oncogene.* 1996;13(4):813-22.

71. Bochenek ML, et al. Ephrin-B2 regulates endothelial cell morphology and motility independently of Eph-receptor binding. *J Cell Sci.* 2010;123(Pt 8):1235-46.

72. Frye M, et al. EphrinB2-EphB4 signalling provides Rho-mediated homeostatic control of lymphatic endothelial cell junction integrity. *eLife.* 2020;9.

73. Hirschberg RM, et al. Electron microscopy of cultured angiogenic endothelial cells. *Microsc Res Tech.* 2005;67(5):248-59.

74. Dong M, et al. Spatiomechanical Modulation of EphB4-Ephrin-B2 Signaling in Neural Stem Cell Differentiation. *Biophysical journal.* 2018;115(5):865-73.

75. Jurisic G, et al. An unexpected role of semaphorin3a-neuropilin-1 signaling in lymphatic vessel maturation and valve formation. *Circ Res.* 2012;111(4):426-36.

76. Bouvree K, et al. Semaphorin3A, Neuropilin-1, and PlexinA1 are required for lymphatic valve formation. *Circ Res.* 2012;111(4):437-45.

77. Petrova TV, et al. Defective valves and abnormal mural cell recruitment underlie lymphatic vascular failure in lymphedema distichiasis. *Nature Medicine.* 2004;10(9):974-81.

78. Sarin S, et al. Duplex ultrasonography for assessment of venous valvular function of the lower limb. *Br J Surg.* 1994;81(11):1591-5.

79. Lurie F, et al. Multicenter assessment of venous reflux by duplex ultrasound. *J Vasc Surg.* 2012;55(2):437-45.

80. van Bemmelen PS, et al. Quantitative segmental evaluation of venous valvular reflux with duplex ultrasound scanning. *J Vasc Surg.* 1989;10(4):425-31.

81. Maurins U, et al. Distribution and prevalence of reflux in the superficial and deep venous system in the general population--results from the Bonn Vein Study, Germany. *J Vasc Surg.* 2008;48(3):680-7.

82. Muzumdar MD, et al. A global double-fluorescent Cre reporter mouse. *Genesis.* 2007;45(9):593-605.

83. Grunwald IC, et al. Hippocampal plasticity requires postsynaptic ephrinBs. *Nature neuroscience.* 2004;7(1):33-40.

84. Davy A, and Soriano P. Ephrin-B2 forward signaling regulates somite patterning and neural crest cell development. *Dev Biol.* 2007;304(1):182-93.

85. Venable JH, and Coggeshall R. A Simplified Lead Citrate Stain for Use in Electron Microscopy. *J Cell Biol.* 1965;25:407-8.

935 **Figure 1**

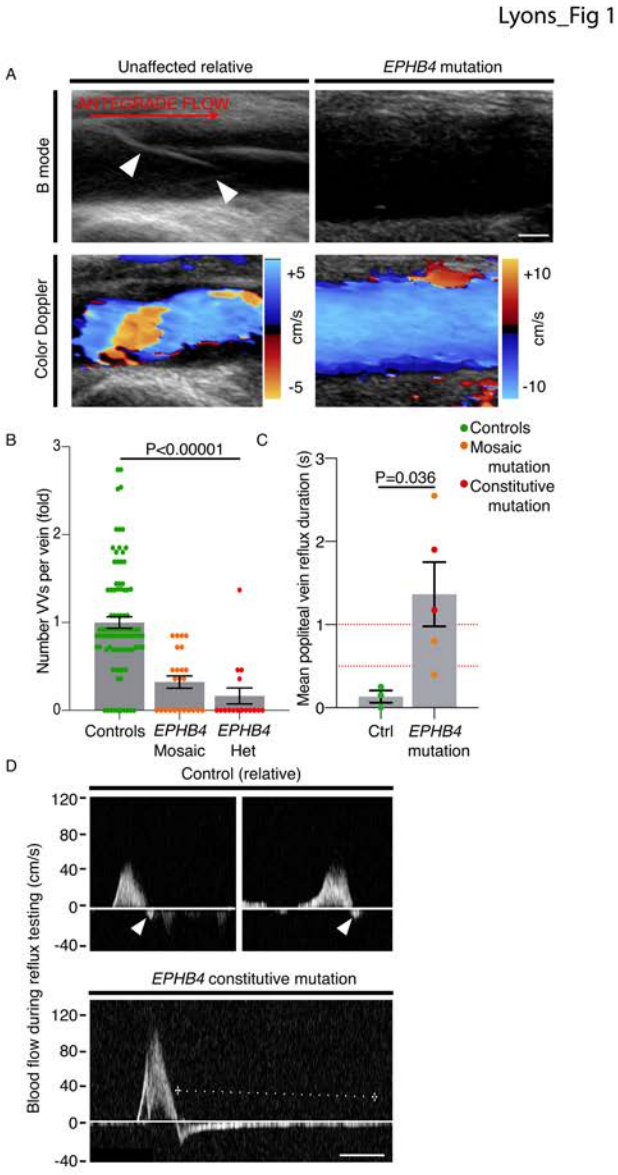

936

937

Figure 1: EPHB4 mutations cause human VV failure

A) VVs (arrowheads) were readily identifiable in the veins of controls, including an unaffected relative, but were rare in patients with a mutation in *EPHB4*. B-mode and color doppler images are shown of the popliteal vein. Blood flow left to right, velocity indicated by color scale. Bar=2mm

B) Fewer VVs per vein were seen in participants with mosaic or constitutive (heterozygous) *EPHB4* mutation (P=1.7x10-11, ANOVA). N=92 veins in 13 controls, and 40 veins in 5 patients with *EPHB4* mutation (mosaic or constitutive). Data points represent individual veins. Het = heterozygous.

C) Popliteal (deep) venous reflux was identified in mosaic and constitutive carriers of *EPHB4* mutations (P=0.036, Mann-Whitney). Blood velocity ≥0.5s indicates reflux and ≥1s indicates severe reflux (red dotted lines). Data points represent mean of left and right popliteal reflux duration for each individual.

D) Representative blood velocity in the popliteal vein during reflux testing is shown for an unaffected relative (with no significant reflux, arrowheads) and a patient carrying an *EPHB4* mutation, demonstrating significant deep venous reflux (dotted line = 2.14s, bar=500ms). Throughout all figures, antegrade blood flow is from left to right. Error bars indicate SEM.

961 **Figure 2**

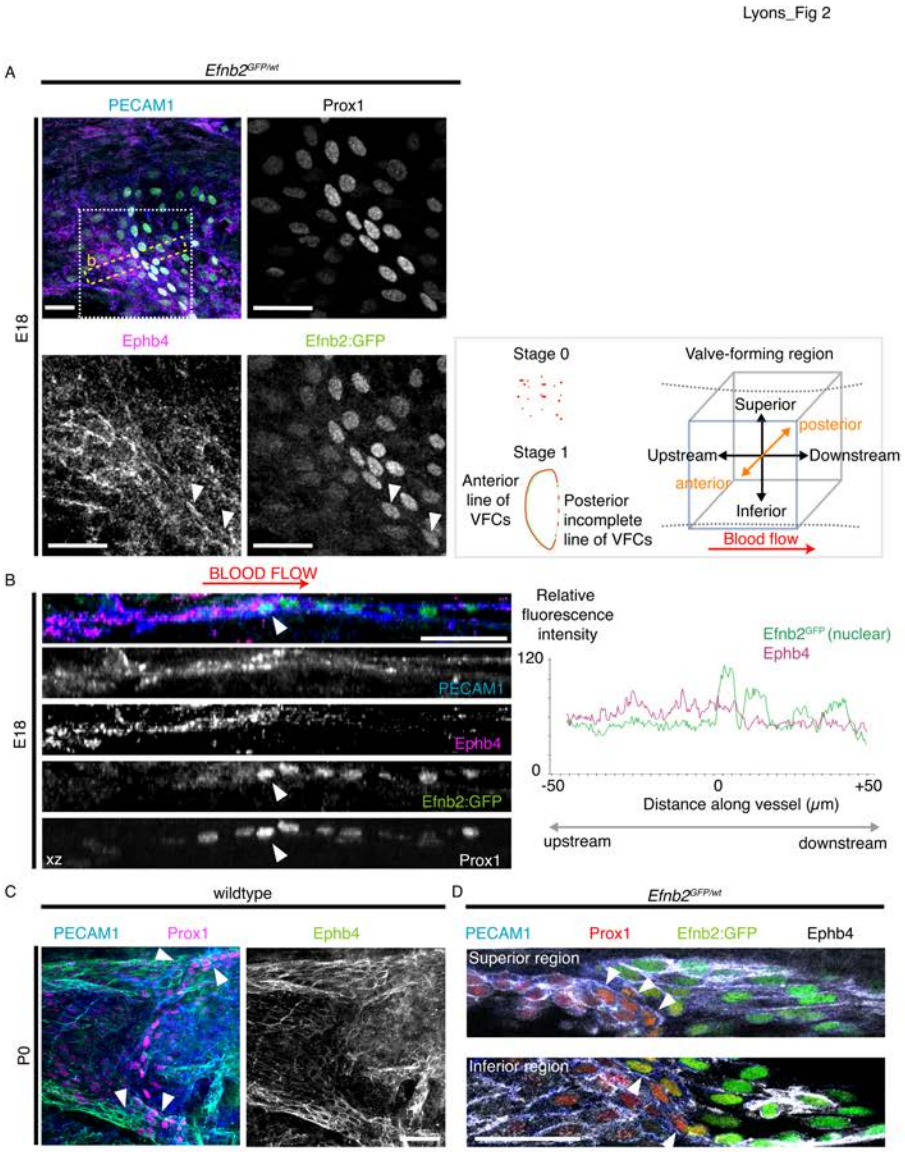

962

963

Figure 2: Expression of EphB4 in Efnb2GFP reporter E18 and P0

A) Localisation of PECAM1 (blue), Ephb4 (magenta), and Prox1 (white), Efnb2:GFP (green) in heterozygous Efnb2GFP mice at E18. Part of an E18 VV is shown, and the white boxed area (which contains organizing VFCs) is shown enlarged in single channel images. Only the anterior vein wall is shown. Arrowhead indicates a VFC nearer the inferior edge of the vessel co-expressing Ephb4 and Efnb2GFP. The schematic indicates stages 0 and 1 of VV development, as previously defined in Ref 11. Red=Prox1hi VFCs, which form a continuous line across the anterior vein wall at stage 1. The orientation of all confocal z-stacks is indicated and is the same throughout all figures. wt = wildtype.

B) An XZ projection (13.6μm deep), and the fluorescence intensity profile for Efnb2GFP and EphB4 is shown across the organizing VFCs, indicated by the yellow boxed area in A. The EphB4 signal is stronger upstream (to the left) of the VFCs (indicated by arrowheads, or “0” on the graph x axis), whilst the Efnb2GFP signal is stronger in VFCs and downstream. ($P<0.0001$, N=6 VV, T test). The multichannel image does not include Prox1.

C) In wildtype VVs at P0, Prox1hi VFCs expressed EphB4, and it was particularly strongly expressed in the superior and inferior areas of the vein (arrowheads).

D) Co-expression of Ephb4 and Efnb2 was confirmed in *Efnb2GFP* mice. 6μm z-projections of the upper and lower regions of a valve are shown. Arrowheads indicate reorientated VFCs (orange). (Uncropped images are provided in Supplementary Figure 2B). Bars = 20μm

988 **Figure 3**

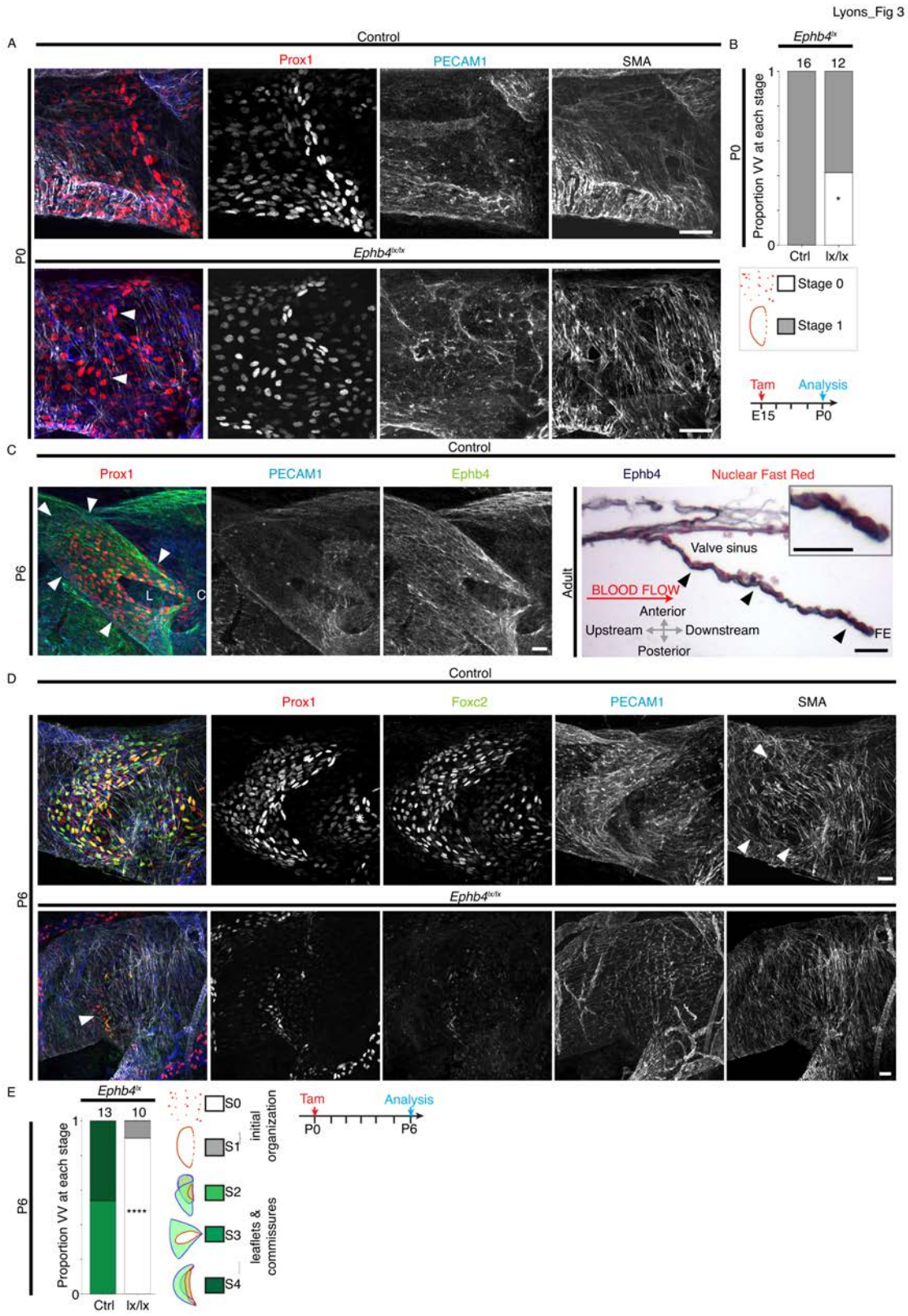

989
990

Figure 3: EphB4 is expressed at E18 and P0 and is required for normal VFC organization, and leaflet development to P6

A-B) Homozygous deletion of *Ephb4* at E15 (analysed at P0) resulted in disrupted organization of VFCs, similar to deletion of *Efnb2*, albeit some VVs appeared to develop normally. The number of VVs analysed for each condition is indicated above each bar in the chart. *=P0.008, Fisher's Exact test. Bars = 20μm. Tam = Tamoxifen, SMA = smooth muscle alpha actin

C) EphB4 was localised in wildtype P6 VVs and surrounding vein. The leaflet of a stage 3 VV is indicated by arrowheads. L=valve lumen and C=the single commissure. In adult VV, longitudinal sections were prepared, and EphB4 (dark blue stain) was most strongly localised to the luminal surface of VV leaflets (black arrowheads) and leaflet free edge (FE, enlarged in inset). The counterstain is Nuclear Fast Red. Arrows indicate the orientation of the adult histological section only (all confocal images are oriented as shown in Fig.2).

D-E) Induction of homozygous *Ephb4* deletion at P0 with Tamoxifen (analysis at P6) resulted in entirely absent VV leaflets, and failure to remodel the surrounding SMCs (arrowheads in upper panel), at P6. Only a few Prox1hi/Foxc2hi cells remained (arrowhead in lower panel). ∗ indicates a downstream tributary valve.

E) Bar chart shows the proportion of VVs identified at each stage, with stage and colour indicated in adjacent key, at P6 for the indicated genotypes. The number of VVs analysed for each condition is given above each bar.

1016 ****=P<0.00005, Chi Sq vs control, N=13 control VVs vs 10 Ephb4 deleted. Bars in

1017 A,C,D = 20μm

1018

1019

1020 **Figure 4**

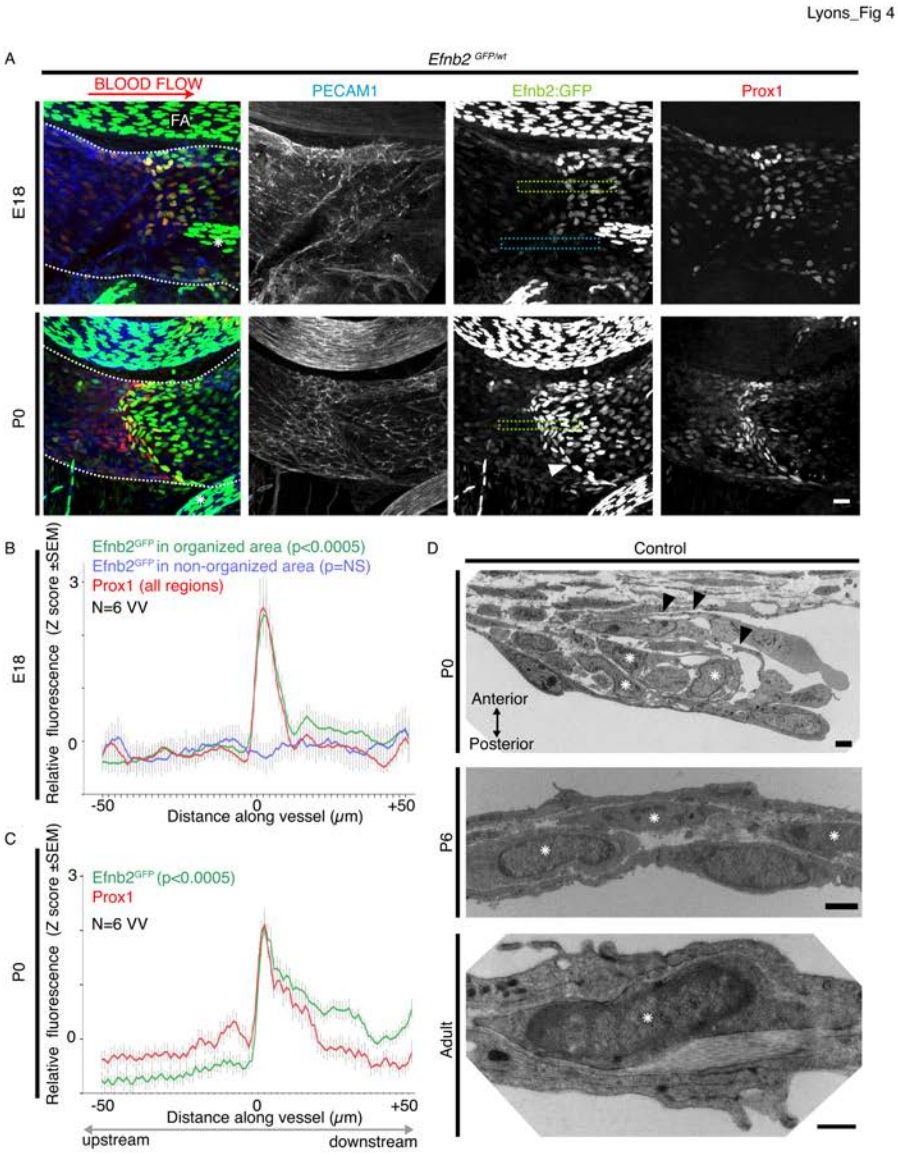

1021
1022

Figure 4: Formation of ephrinB2 expression boundary in VV-forming region

A) Localisation of PECAM1 (blue), Prox1 (red) and Efnb2GFP reporter signal (green, His-tagged and therefore nuclear) at E18 and P0 in heterozygous Efnb2GFP mice. Wholemount preparation of the proximal femoral vein is shown. At E18 there was partial, and variable, organization of VFCs. For example, in the superior area of the VV-forming region but not the inferior area. Those areas with organization at E18 showed a weak Efnb2GFP expression boundary, which was clearer at P0 (white arrowhead). Dotted lines indicate the femoral vein boundary, adjacent to the femoral artery (FA). As expected, arterial ECs showed stronger Efnb2GFP signal. ∗ indicates an overlying arterial branch (cut).

B-C) At E18, analysis of the relative fluorescence intensity across developing valves revealed a peak in Efnb2GFP signal (green line) coincident with that of Prox1hi (red) VFCs in organizing areas, but not in adjacent areas that are not yet organized (blue line). At both E18 and P0, Efnb2GFP signal is stronger downstream, and this difference is more apparent at P0. Mean of 6 VVs and 7-12 regions analysed per VV and representative regions analysed are shown boxed (green, blue) in A. P values in B,C are T tests comparing Efnb2GFP proximal and distal to the VFC leading edge. NS = not significant.

D) TEM analysis at P0 showed rotated VFCs detached from underlying basement membrane (arrowheads). Interstitial cells (∗) populated the developing leaflet core, and persisted at P6 and in adults. TEM micrographs are orientated at 90^{o} to confocal images, as indicated by arrows at P0 in D. Further examples of interstitial cells (in murine and human VVs) are shown in Supplementary Figure 3.

N≥6 VV and blood flow left to right at all time points and in B,C. Bar = 20μm in A; and in D Bar = 2μm at P0-P6, 500nm in Adult.

1052 **Figure 5**

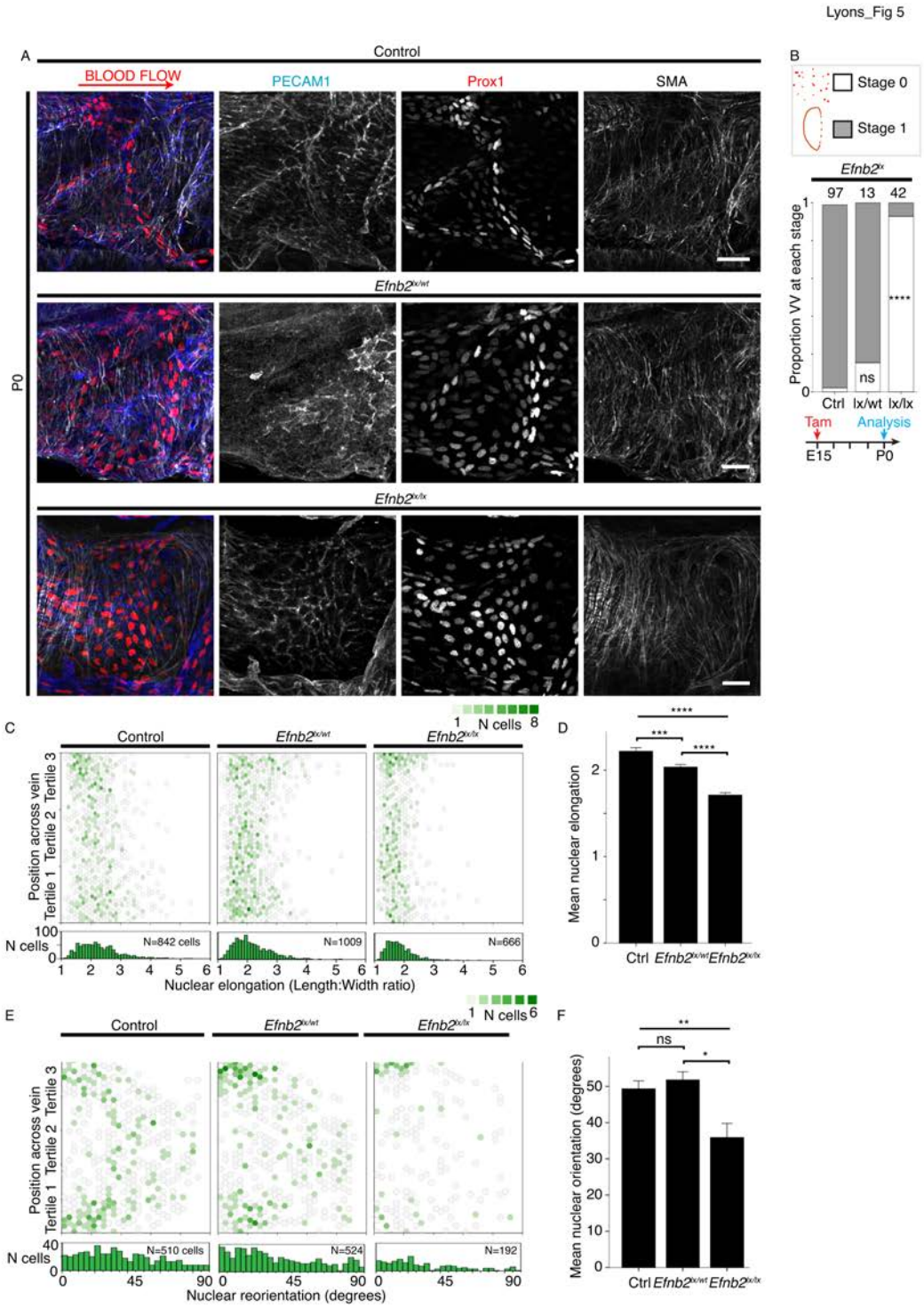

1053
1054

Figure 5: Effect of *Efnb2* deletion on organization of VFCs

A,B) Localisation of PECAM1 (blue), Prox1 (red) and SMA (white) in littermate controls, heterozygous (*Efnb2lx/wt*) and homozygous (*Efnb2lx/lx*) mice at P0, following Tamoxifen induction of Efnb2 deletion at E15. In controls and *Efnb2lx/wt* mice valves reached stage 1 of development, as normal. Homozygous deletion resulted in a failure to organize normally, with Prox1hi cells distributed over a wider upstream-downstream area of the vein, and failure of VFCs to elongate and reorientate.

B) The bar chart shows the proportion of VVs identified at stage 0 (white) and stage 1 (grey) at P0 for the indicated genotypes, and the number of VVs analysed for each condition is given above each bar. P values derive from two-sided Fisher's Exact test vs control.

C) Hex-binned scatterplot of VFC elongation (length/width ratio) across the vein from superior to inferior. N=2517 cells, ≥6 VVs.

D) Bar chart (±sem) summarising the results from (C) showing that both heterozygous and homozygous deletion resulted in significant reductions in VFC elongation. ANOVA with Bonferroni post hoc. For between groups ANOVA, F=109 with 2df, P=3.2x10-46.

E) Hex-binned scatterplot of VFC reorientation (in VFCs with nuclear length:width ratio ≥2) across the vein from superior to inferior. N=1226 cells, ≥6 VVs. After homozygous deletion, the VFCs with correctly reorientated nuclei were lost, particularly in the centre of the vessel.

F) Bar chart (±sem) summarising the results from (E). Homozygous deletion resulted in significantly reduced reorientation. ANOVA with Bonferroni post hoc. For ANOVA,

1080 F=7.1 with 2df, P=0.0009. *=P<0.05, **=P<0.005, ***P<0.0005, ****=P<0.00005.

1081 Bars = 20μm

1082

1083

1084 **Figure 6**

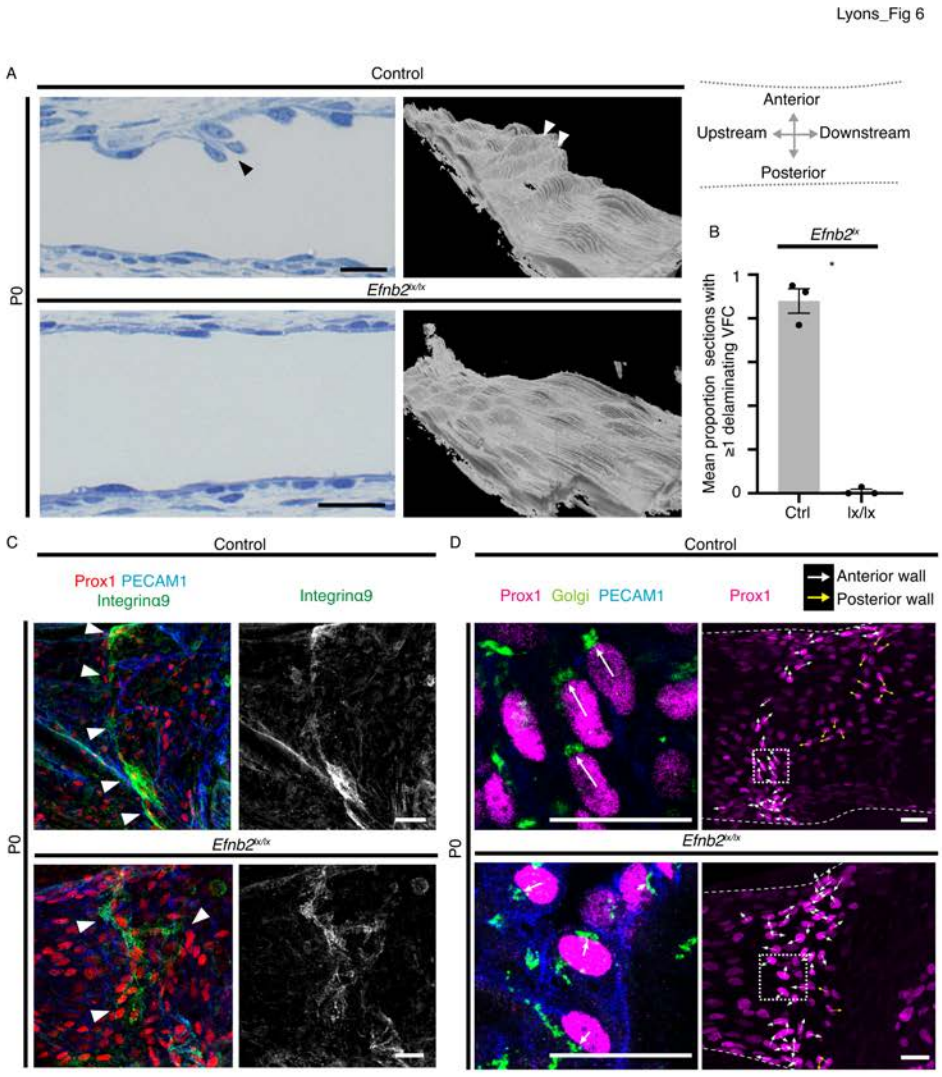

1085
1086

Figure 6: Failure of VFCs to project into vessel lumen and abnormal integrin expression

A) Semi-thin longitudinal sections of P0 femoral veins showed protruding VFCs in littermate controls, but no protruding cells were seen after homozygous *Efnb2* deletion. 3D reconstructions of semi-thin sections show protruding VFCs (arrowheads) in controls only. The schematic indicates the orientation of the semi-thin sections.

B) A significant reduction in the mean number of sections showing protruding cells was identified. (≥60 sections were analysed per sample, T test, N=3 VV per group, error bars indicate SEM).

C) Integrinα9 was expressed in a ring around the organized VFCs in littermate controls (white arrowheads), but after homozygous *Efnb2* deletion, the localisation of integrinα9 expression was disrupted and chaotic ($P<0.05$, Chi Square test of the proportion of VVs showing normal vs disrupted integrinα9 expression pattern, N≥6 VV per group)

D) VFC polarity (indicated by white arrows) was examined by co-staining for Prox1 (magenta), PECAM1 (blue) and Golgi (green). Polarity was determined for individual VFCs using 0.5μm sections, and a z-projection of 2-4 confocal sections shown on the right (area enlarged outlined by dotted box,). In littermate controls, cells in the central region of the vein were aligned with the line of organized VFCs, whilst after homozygous *Efnb2* deletion, cell alignment was chaotic. $P<0.05$, Chi Square test of

1112 the proportion of VVs showing normal vs chaotic VFC alignment, N≥8 VV per group.
1113 Yellow arrows indicate VFCs on the posterior vein wall. Bars in A,C,D 20μm. C and D
1114 are oriented as shown in Fig.2A.
1115
1116

Figure 7

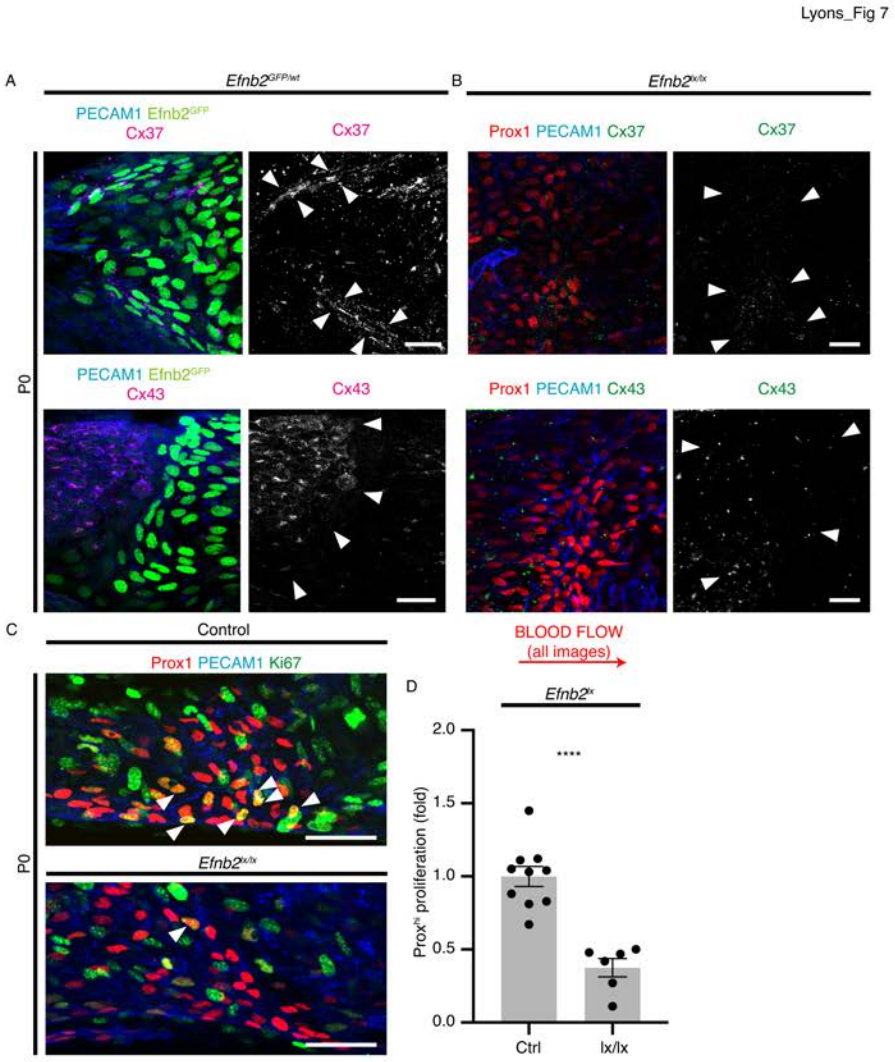
Lyons_Fig 7
A
Efnb2GFP/wt
B
Efnb2lx/lx
PECAM1 Efnb2GFP
Cx37
Cx37
Prox1 PECAM1 Cx37
Cx37
P0
PECAM1 Efnb2GFP
Cx43
Cx43
Prox1 PECAM1 Cx43
Cx43
C
Control
Prox1 PECAM1 Ki67
P0
Efnb2lx/lx
BLOOD FLOW
(all images)
D
Efnb2lx
****
Prox+ proliferation (fold)
2.0
1.5
1.0
0.5
0.0
Ctrl
lx/lx

Figure 7: *Efnb2* deletion disrupts gap junction protein expression pattern, and proliferation

A) Localisation of PECAM1 (blue), and either Cx37 or Cx43, as indicated (magenta) around VFCs at P0 in heterozygous Efnb2GFP (green) mice. As expected, at P0 Cx37 was localised to Efnb2GFP-expressing VFCs, primarily forming large gap junction plaques (examples indicated between arrowheads) and Cx43 was localised to endothelium upstream of these VFCs (region to the left of the arrowheads). Smaller plaques are also identifiable.

B) Localisation of PECAM1 (blue), Prox1 (red) and either Cx37 or Cx43, as indicated (green), after homozygous deletion of *Efnb2*. The tightly regulated expression pattern of Cx37 was disrupted, with expression over a wider area (arrowheads) and the typical appearance of larger plaques was lost. The expression pattern of Cx43 was also disrupted and no longer confined to upstream of VFCs (arrowheads). ($P<0.05$, Chi Square test of the proportion of VVs showing normal (confined) vs disrupted expression pattern, N≥6 VV per group).

C-D) The proportion of proliferating VFCs was assessed by colocalisation of Prox1 and Ki67 (arrowheads). Ki67+ve VFCs were easily identified in littermate controls, but far fewer proliferating VFCs were identifiable after homozygous *Efnb2* deletion. The inferior region of the vein is shown. ($P<0.00005$, unpaired T test, N≥6 VV per group, error bars indicate SEM). Bars in A-C = 20μm